

# Identification of Phyllosoma Larvae of the Lobsters *Acantharctus* and *Biarctus* (Crustacea: Scyllaridae) from the SW Indian Ocean

Rebeca Genis-Armero<sup>1</sup>, Johan Groeneveld<sup>2,3</sup>, Sohana Singh<sup>2</sup>, Paul F. Clark<sup>4</sup>, Laure Corbari<sup>5</sup>, and Ferran Palero<sup>1,4,\*</sup>

<sup>1</sup>Cavanilles Institute of Biodiversity and Evolutionary Biology, University of Valencia, Paterna, Spain.

\*Correspondence: E-mail: crustomics@gmail.com (Palero)

E-mail: rebeca92grj@gmail.com (Genis-Armero)

<sup>2</sup>Oceanographic Research Institute, Durban, South Africa. E-mail: jgroeneveld@ori.org.za (Groeneveld); ssingh@ori.org.za (Singh)

<sup>3</sup>School of Life Sciences, University of KwaZulu-Natal, Pietermaritzburg, South Africa

<sup>4</sup>Department of Life Sciences, The Natural History Museum, Cromwell Road, London SW7 5BD, England. E-mail: p.clark@nhm.ac.uk (Clark)

<sup>5</sup>UMR 7205 ISYEB, Équipe "Explorations, Espèces et Spéciations", Muséum National d'Histoire Naturelle, Paris, France.

E-mail: corbari@mnhn.fr (Corbari)

Received 5 October 2022 / Accepted 29 April 2023 / Published 26 July 2023

Communicated by Benny K.K. Chan

The accurate assignment of cryptic larvae to species-level is a key aspect of marine ecological research and can be achieved through integrated molecular and morphological studies. A combination of two mitochondrial markers (COI and 16S) and a detailed morphological analysis was used to identify phyllosoma larvae of slipper lobster (Scyllaridae) species collected during a survey in the SW Indian Ocean. Two morphotypes were tentatively assigned to *Acantharctus ornatus* and *Biarctus pumilus*, both genera for which the larval morphology was unknown. Morphological revision of an adult specimen used to generate the putative *A. ornatus* sequences in GenBank revealed that it was misidentified and corresponds to *B. dubius*. The final phyllosoma stage of *B. pumilus* and subfinal and final stages of *A. ornatus* were described, clarifying prior misidentifications in the literature. Scyllarid biodiversity in the SW Indian Ocean is underestimated and sampling of deeper water layers is recommended to complete current knowledge of species and larval stages present in the region.

**Key words:** SW Indian Ocean, South Africa, KwaZulu-Natal Bight, Phyllosomas, Morphological description

## BACKGROUND

Scyllaridae Latreille, 1825 is one of the most speciose of all marine lobster families and contains some 20 genera and at least 89 species (Yang et al. 2012; Chan 2019). Slipper lobsters occur in tropical and temperate habitats, from shallow coastal to upper slope depths, and on hard and soft substrates (Holthuis 2002). Scientific information on slipper lobsters has increased over the past two decades but is confined to a few species with importance to fisheries (Lavalli et al. 2019). The dispersal phase of slipper lobsters as drifting

larvae, called phyllosoma, is poorly understood beyond descriptive information (Booth et al. 2005). Phyllosomas are cryptic, moult through multiple developmental stages and are widely distributed in coastal and offshore waters (Palero et al. 2014).

Emmerson (2016) listed 15 slipper lobster species from southern Africa, of which 13 were present as adults along the subtropical southeast coast, a region influenced by tropical Western Indian Ocean waters. The phyllosomas of only six of these species have been described: *Scyllarides squammosus* (H. Milne Edwards, 1837); *Ibacus novemdentatus* Gibbes, 1850;

*Parribacus antarcticus* (Lund, 1793); *Chelarctus cultrifer* (Ortmann, 1897); *Eduarctus martensii* (Pfeffer, 1881) and *Petrarctus rugosus* (H. Milne Edwards, 1837) (von Bonde 1930; Robertson 1969; Berry 1974; Marinovic et al. 1994; Higa and Shokita 2004; Wakabayashi et al. 2012 2017; Palero et al. 2014 2016). Berry (1974) undertook a comprehensive study of > 2350 phyllosomas collected off the coast of eastern South Africa during surveys from 1970 to 1973. Based on morphology keys, expected distribution ranges and larval size, 95% of 1965 slipper lobster phyllosomas were tentatively assigned to *Scyllarus rugosus* (now *P. rugosus*) followed by 4.5% to *Scyllarus martensii* (now *E. martensii*). Several other species (e.g., *S. squamosus*, *P. antarcticus* and *I. novemdentatus*) were present in low numbers.

The advent of DNA barcoding has substantially improved larval identification over the past two decades (Palero et al. 2009b; Wakabayashi et al. 2020; Ueda et al. 2021; Genis-Armero et al. 2022; Hidaka et al. 2022). Even so, species without barcode records, misidentifications in barcode reference libraries, and incomplete taxonomic information impose limitations on DNA-based identification (Singh et al. 2021). Molecular results have further shown that historical larval assignments based on morphology can be unreliable (Palero et al. 2008 2011). The phyllosoma stages of several genera occurring in the SW Indian Ocean remain unknown or have previously been attributed to other genera (e.g., *Biarctus* Holthuis, 2002 and *Acantharctus* Holthuis, 2002) (Berry 1974; Wakabayashi et al. 2020). In the present study, an integrative taxonomy approach that combined two mitochondrial markers COI (cytochrome *c* oxidase subunit I) and 16S (RNA component of the mitochondrial ribosome) and a thorough morphological analysis is used to identify slipper lobster phyllosomas collected during a ship-based survey off eastern South Africa.

## MATERIALS AND METHODS

### Study site

A survey undertaken by the RV *Dr Fridtjof Nansen* (Michalsen et al. 2018) collected phyllosomas along the eastern coast of South Africa in January and February 2018 (Fig. 1). Manta nets (375  $\mu$ m mesh, 0.19  $\times$  0.61 m [H  $\times$  W]) and ring nets (500  $\mu$ m mesh, 0.8 m diameter) were towed in surface waters (0–5 m from the surface) for 5 minutes at a speed of 3 knots at 22 sampling stations between Port St Johns in the southwest and St Lucia in the northeast. Stations were

located at depth isobaths between 26 and 1054 m, thus covering the width of the continental shelf and upper slope, and most stations were sampled with both nets. Phyllosomas were obtained from three out of a total of 35 tows, at neighbouring sampling stations in the northern KwaZulu-Natal (KZN) Bight, at 32 m and 99 m depth isobaths (Fig. 1). Phyllosomas were picked out of the tow net samples and individually preserved in vials with 96% ethanol and stored at -20°C.

### Sampling

A total of 143 phyllosomas were photographed and tentatively classified to species and developmental stage. Photographs of the specimens allowed one of the authors (FP) to recognize two different morphotypes and a pre-selection of 24 phyllosomas were sent to the laboratory at the Cavanilles Institute of Biodiversity and Evolutionary Biology (Valencia, Spain) for more detailed morphological and molecular analyses (Table 1). Unfortunately, the specimen in a middle stage (stage V) was damaged during transport and could not be described. A preliminary investigation using DNA barcoding found no direct match for the larvae on GenBank, because no reference sequences were available in public records. Based on morphological similarities to putative phyllosomas of *A. posteli* from Mauritania (see Discussion), type material of both *A. posteli* (MNHN-IU-2013-14854 and MNHN-IU-2013-14855) and *S. paradoxus* (MNHN-IU-2013-14844 and MNHN-IU-2013-14845) was obtained from the crustacean collections of the Muséum national d'Histoire naturelle, Paris, for comparison.

### DNA analyses

Total genomic DNA extractions were performed on a subset of larvae and the adult type material from MNHN (see Table 2) using the Chelex-resin method (Palero et al. 2010). Standard universal primers for two mitochondrial genes (COI and 16S) were used following previous studies on lobster phylogenetics and DNA barcoding of phyllosoma larvae (Palero et al. 2008 2009a; Bracken-Grissom et al. 2014; Genis-Armero et al. 2019). Polymerase chain reaction amplifications used ~30 ng of genomic DNA in a reaction containing 1 U of Taq polymerase (Amersham), 1  $\times$  buffer (Amersham), 0.2 mM of each primer and 0.12 mM dNTPs. The thermal profile was 94°C for 4 min for initial denaturation, followed by 30 cycles of 94°C for 30 s, 50°C for 30 s, 72°C for 30 s and a final extension at 72°C for 4 min. Sequences were obtained using the Big-Dye Ready-Reaction kit ver. 3.1 (Applied Biosystems) on an ABI Prism 3770 automated sequencer at the

NHM sequencing facilities. Chromatograms for each DNA sequence were checked with BioEdit v7.2.5 (Hall 1999) and sequence alignment was conducted using the program Muscle v3.6 (Edgar 2004) with default parameters. Model selection was performed according to the BIC criterion as implemented in MEGA X (Tamura et al. 2021). The maximum-likelihood (ML) phylogenetic tree construction method was applied as implemented in PhyML v3.0 (Guindon et al. 2010). Initial trees for the heuristic search were obtained automatically by applying the Neighbour-Joining algorithm to a matrix of pairwise distances

estimated using the Maximum Composite Likelihood approach, then selecting the topology with a superior log-likelihood value. Nodal support was assessed using 1000 bootstrap replicates.

**Morphological description**

Following the developmental stage classification of Robertson (1971), 23 specimens were assigned to subfinal (VIII) and final (IX) stages (Table 2). Moreover, another specimen was tentatively assigned to an intermediate stage (VI), but it was not used for

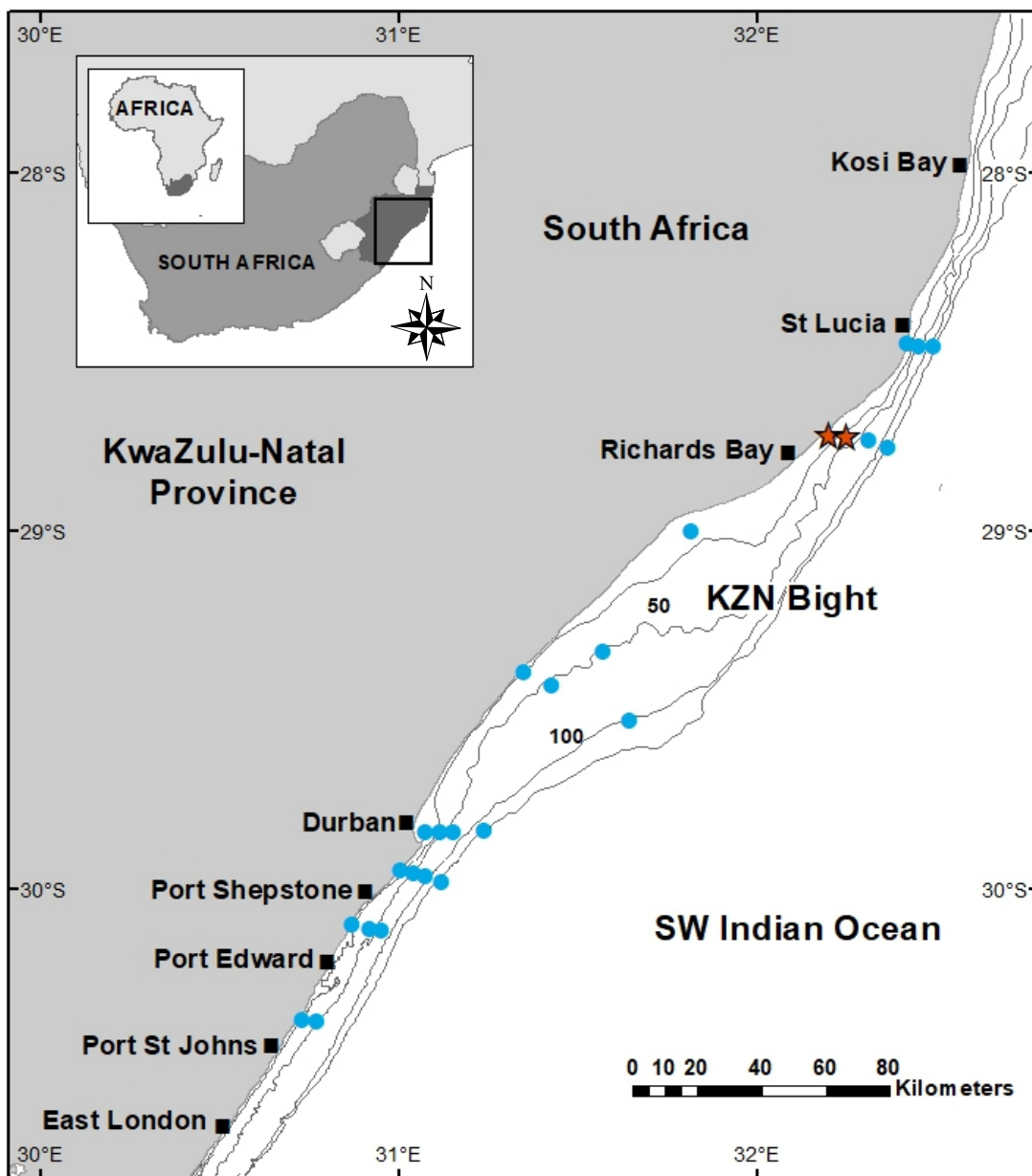


Fig. 1. Location of 22 stations sampled by the RV *Dr Fridtjof Nansen* along the KwaZulu-Natal coast in eastern South Africa. Stations where phyllosomas were caught are indicated with a star.

description because of its poor condition. Drawings of larvae and their appendages were made with a camera lucida attached to a Leica M165C high-performance stereo microscope (Leica Microsystems, Germany). Digitization of drawings was carried out using an Intuous-S graphic tablet (Wacom) and Adobe

Illustrator (<https://adobe.com/products/illustrator>) following Coleman (2003 2009). The sequence of larval descriptions was based on the malacostraca somite plan and described from anterior to posterior and proximal to distal (Clark et al. 1998; Clark and Cuesta 2015). The term biramous was considered inappropriate for the

**Table 1.** Phyllosoma larvae collected during the Nansen survey. Sampling information includes stage, date, station, geographical coordinates, net deployed and number of larvae captured. Selected specimens sent to Valencia are indicated in bold

Morphotype	Stage	Date	Station	Latitude	Longitude	Net	N° larvae
A	Final	2018/2/3	56	-28.76	32.21	Manta	2 <b>(2)</b>
B	Final	2018/2/2	56	-28.76	32.21	Manta	2
		2018/2/3				Manta	43 <b>(15)</b>
						Ring	7 <b>(1)</b>
	Subfinal					Manta	36 <b>(4)</b>
						Ring	39 <b>(1)</b>
	VII					Manta	1
	VI					Manta	1
	V					Ring	1 <b>(1)</b>
	Final		58	-28.8	32.33	Ring	2
	Subfinal					Ring	9

**Table 2.** Morphological measurements (BL, CL, CW, TL, TW, PL, PW) and ratios (BL/CW and CW/TW) obtained from the selected phyllosoma used for descriptions. Morphotype, most likely species assignment, voucher code, and developmental stage are also shown. \*DNA barcoded phyllosoma

Most likely identification	Morphotype	Voucher Code	Stage	BL	CL	CW	TL	TW	PL	PW	BL/CW	CW/TW
<i>Biarctus pumilus</i>	A	<b>Manta_L39*</b>	Final	12.1	6.7	6.6	3.3	4.1	2.8	2.8	1.8	1.6
<i>Biarctus pumilus</i>	A	<b>Manta_L80*</b>	Final	13.0	7.5	7.2	4.0	4.5	3.2	2.9	1.8	1.6
<i>Acantharctus ornatus</i>	B	<b>Ring_L32*</b>	V	6.3	4.4	4.5	2.1	2.2	0.6	0.6	1.4	2.0
<i>Acantharctus ornatus</i>	B	<b>Manta_L30*</b>	Subfinal	9.1	5.9	6.1	2.9	3.0	1.4	1.4	1.5	2.1
<i>Acantharctus ornatus</i>	B	Manta_L31	Subfinal	11.0	7.2	7.1	3.6	3.8	1.8	2.0	1.5	1.9
<i>Acantharctus ornatus</i>	B	<b>Ring_L08*</b>	Subfinal	11.3	7.2	7.5	3.4	3.6	2.0	2.2	1.5	2.1
<i>Acantharctus ornatus</i>	B	Manta_L52	Subfinal	11.7	7.5	7.6	4.0	3.8	2.1	2.1	1.5	2.0
<i>Acantharctus ornatus</i>	B	<b>Manta_L01*</b>	Subfinal	11.9	7.9	8.3	2.8	3.2	1.8	1.9	1.4	2.6
<i>Acantharctus ornatus</i>	B	Manta_L79	Final	13.7	7.6	-	4.1	4.9	3.7	3.2	-	-
<i>Acantharctus ornatus</i>	B	Manta_L82	Final	13.9	8.2	8.2	3.6	4.5	3.8	3.1	1.7	1.8
<i>Acantharctus ornatus</i>	B	Manta_L33	Final	14.4	8.5	8.8	4.2	4.7	3.6	3.2	1.6	1.9
<i>Acantharctus ornatus</i>	B	Manta_L43	Final	14.5	8.6	8.8	4.2	4.8	3.7	3.3	1.6	1.9
<i>Acantharctus ornatus</i>	B	Manta_L76	Final	14.7	8.8	8.6	3.9	4.8	3.7	3.1	1.7	1.8
<i>Acantharctus ornatus</i>	B	<b>Manta_L62*</b>	Final	14.7	8.7	8.9	4.0	4.8	3.5	3.3	1.7	1.9
<i>Acantharctus ornatus</i>	B	Manta_L44	Final	14.9	8.7	8.9	4.0	4.8	3.9	3.3	1.7	1.8
<i>Acantharctus ornatus</i>	B	Manta_L70	Final	15.2	9.0	9.5	4.3	5.1	3.6	3.3	1.6	1.9
<i>Acantharctus ornatus</i>	B	Manta_L73	Final	15.2	9.0	9.3	4.0	4.9	3.7	3.3	1.6	1.9
<i>Acantharctus ornatus</i>	B	Manta_L69	Final	15.4	9.1	9.1	4.4	5.0	3.8	3.6	1.7	1.8
<i>Acantharctus ornatus</i>	B	Manta_L72	Final	15.5	9.0	9.3	4.4	5.1	4.0	3.5	1.7	1.8
<i>Acantharctus ornatus</i>	B	Manta_L48	Final	15.7	9.5	9.4	4.4	5.2	3.8	3.5	1.7	1.8
<i>Acantharctus ornatus</i>	B	Manta_L40	Final	15.7	9.2	9.2	4.7	5.1	3.8	3.4	1.7	1.8
<i>Acantharctus ornatus</i>	B	<b>Manta_L41*</b>	Final	16.0	9.3	9.6	4.2	5.2	4.0	3.4	1.7	1.8
<i>Acantharctus ornatus</i>	B	Ring_L031	Final	16.5	9.2	9.9	4.7	5.1	4.3	3.7	1.7	1.9
<i>Acantharctus ornatus</i>	B	<b>Manta_L65*</b>	Final	17.8	10.4	10.2	4.3	5.9	4.6	4.0	1.7	1.7

antennule, and instead of exopod and endopod, primary and accessory flagella were adopted (see Boxshall 2004; Boxshall et al. 2010).

Body length (BL) was measured from the anterior margin of the cephalic shield (between the eyes) to the posterior margin of the telson; cephalic length (CL) from the anterior to posterior margin of the cephalic shield; cephalic width (CW) across the widest part of cephalic shield; thorax length (TL) from the anterior to posterior margin of the thorax; thorax width (TW) across the widest part of the thorax shield; pleon length (PL) from the anterior to posterior margin of the pleon; and pleon width (PW) between the fifth pereopod (P5) coxae. All morphometric measurements were obtained using the software Image J (Schneider et al. 2012). Finally, morphological ratios were obtained for BL/CW, CW/TW and the eyestalk length/antenna length (ES/A2) ratio following previous studies (McWilliam 1995; Lindley et al. 2004; Inoue and Sekiguchi 2006; Genis-

Armero et al. 2022).

## RESULTS

### Molecular analyses

New sequences obtained from the phyllosoma larvae and MNHN adult material have been deposited in GenBank under accession numbers ON964534–ON964541 (COI) and ON960165–ON960178 (16S). The lengths of the gene alignments were 649bp for COI and 511 bp for 16S rDNA. The DNA substitution model selected for the COI alignment was HKY+G+I (lnL = -6130.62), with Gamma parameter (G) of 0.72 and 52% invariant sites, and for the 16S alignment it was TN93+G (lnL = -4012.69) with G of 0.26. The two phylogenetic trees obtained by Maximum Likelihood for COI and 16S (Fig. 2) clustered the most abundant larval

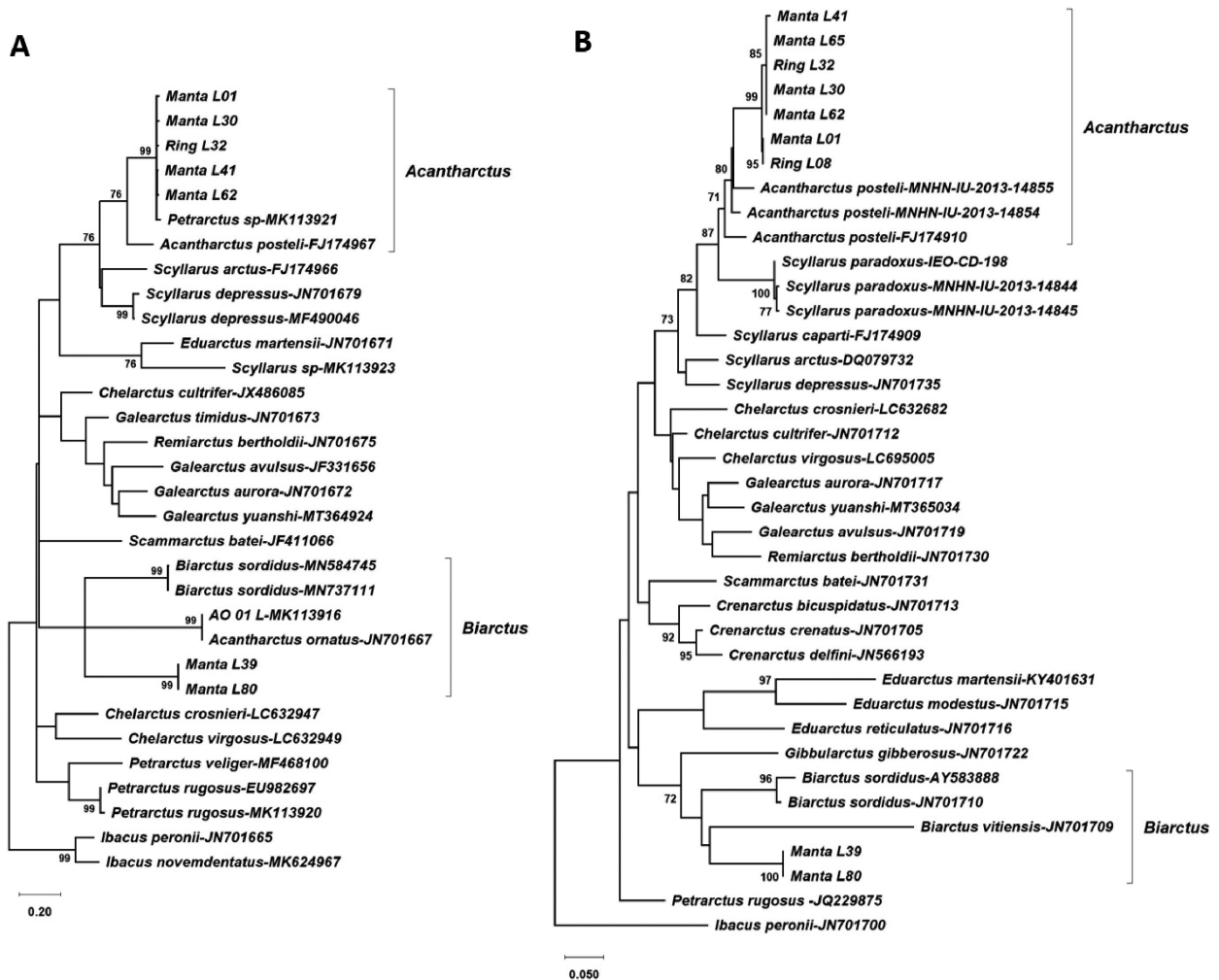


Fig. 2. Maximum likelihood phylogenetic trees obtained from COI (A, left) and 16S (B, right) gene alignments. Only significant bootstrap values (> 70) are shown.

morphotype (see morphotype B in the morphological analysis section below) with *A. posteli*, indicating that they most likely belong to *A. ornatus* (Holthuis, 1960). Moreover, the results obtained also suggested that the putative *A. ornatus* sequences available in GenBank must be misidentified (see below). The sequences of the two other specimens clustered with *Biarctus* COI and 16S rDNA genes, and with sequences of morphotype A in the present study (Fig. 2), although bootstrap support was low.

### Correcting the misidentified *A. ornatus* from GenBank

The pre-existing COI sequences for a putative *A. ornatus* on GenBank (accession numbers JN701667 and MK113916) belong to an adult scyllarid (voucher code WAM C27134) from Dampier Islands (Western Australia) and an undescribed phyllosoma (AO\_01\_L) from eastern South Africa (Govender et al. 2019). Both were confirmed here to be misidentifications

after morphological comparison of the adult museum specimen (WAM C27134) used to produce the sequence in GenBank with *A. ornatus* syntypes (NHMUK 1967.10.2.1-3) and specimens identified by Holthuis (Voucher codes: WAM C8845 and WAM C8846). The latter were collected from Australia but preserved in formaldehyde (Fig. 3). True *A. ornatus* from Australia and syntypes from the Arabian Peninsula (Oman) present a series of diagnostic characters, shared with other *Acantharctus* species (i.e., *A. posteli*), such as the strong spine on the last somite of the thoracic sternum, sharp and pointed teeth on the fourth antennal article and a strong dorsal carina. The WAM C27134 specimen does not present any of these characters and it should be tentatively assigned to *B. dubius* based on the well-developed cardiac and gastric teeth, and a strong anterior submedian carina reaching beyond the gastric tooth. Based on 100% COI sequence similarity to JN701667 on GenBank, the undescribed phyllosoma from eastern South Africa (MK113916; see Govender et al. 2019) was also a *Biarctus*.

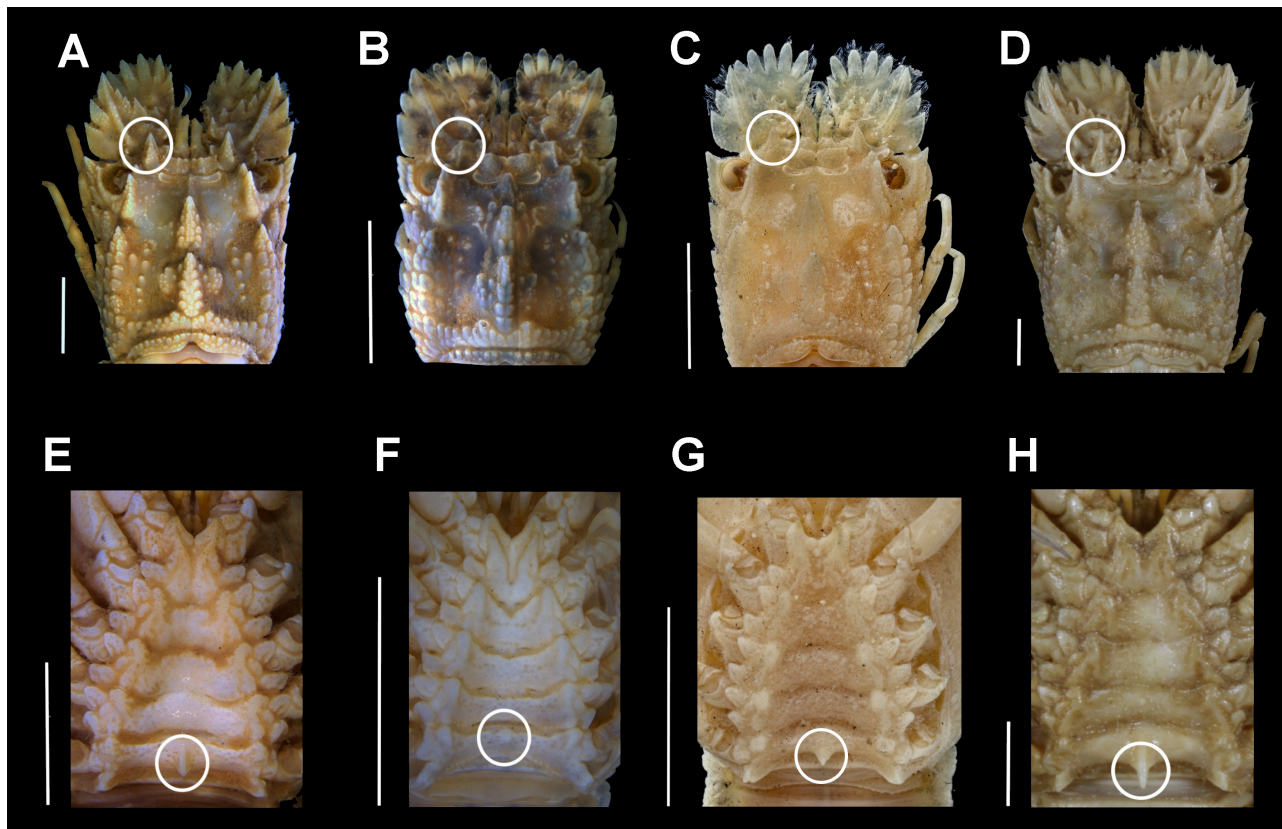


**Fig. 3.** Morphology comparison of the adult slipper lobster labelled as *A. ornatus* in GenBank and true *Acantharctus*. Carapace dorsal view (A–D) and sternum (E–H) for *A. ornatus* from Australia identified by Holthuis (A: WAM C8845, E: WAM C8846); GenBank specimen labelled as *A. ornatus* but being in fact *Biarctus dubius* (B, F: WAM C27134); *A. ornatus* syntype (C, G: 1967.10.1.1-3) and *A. posteli* (D, H: MNHN-IU-2013-14853). The diagnostic characters used to differentiate *Acantharctus* and *Biarctus* (strong dorsal carina and strong spine on the last somite of the thoracic sternum) are indicated with a circle. Scale bars = 5 mm.

## Morphological descriptions of phyllosomas

### Morphotype A – *Biarctus* sp. (probably *Biarctus pumilus*)

Stage IX (Final)  
(Figs. 4–5)

*Material examined:* Manta\_L39; Manta\_L80.

*Morphometrics:* N = 2; BL = 12.09–13.02 mm; CL = 6.71–7.53 mm; CW = 6.63–7.16 mm; TL = 3.25–4.00 mm; TW = 4.47–4.08 mm; PL = 2.84–3.15 mm; PW = 2.94–2.84 mm; BL/CW = 1.8; CW/TW = 1.6; ES/A2 ≤ 0.5.

*Cephalic shield* (Fig. 4A): Rounded shape (CL/CW = 1.0–1.1).

*Eyestalk* (Figs. 4A, 5A): Short (ES/A2 ≤ 0.7).

*Antennule* (Figs. 4A, 5A): Slightly longer than antenna. 3-articled peduncle, article 3 with 3 setae. Primary flagellum with 11–12 rows of sensory setae. Accessory flagellum not articulated, without setae.

*Antenna* (Figs. 4A, 5A): Uniramous and not articulated; slightly shorter than antennule. External lateral margin of endopod expanded medially; distal margin lobated with setae in both margins. Exopod absent.

*Mandibles* (Fig. 5B–C): Asymmetrical dentition, left mandible longer than right. Both mandibles with several small teeth distributed over surface and molar process crowned with many denticles. Right mandible teeth curved towards molar, incisor process with 3 teeth; left mandible teeth elongated, incisor process with 3 teeth. Palp absent.

*Maxillule* (Fig. 5D): Coxal endite with 7 setae, 3 plumidenticulate, 2 long and 1 short; basal endite with 9 setae, 3 serrated. Endopod and exopod absent.

*Maxilla* (Figs. 4A, 5E): Uniramous. Endites and endopod undifferentiated with 2 setae on superior margin of lateral process; exopod (scaphognathite) flattened and expanded, without marginal setae.

*First maxilliped* (Fig. 5E): Uniramous. Endites undifferentiated; endopod present and unarticulated. Exopod absent.

*Second maxilliped* (Figs. 4A, 5F): Biramous. Coxa without setae; basis delimited by exopod bud and 1 seta; endopod with 4 articles, ischium-merus (undifferentiated), carpus, propodus, dactylus with 0, 1, 8–10 and 4–5 setae respectively. Exopod (bud) present.

*Third maxilliped* (Fig. 4A): Uniramous. Gills buds present; 1 pleurobranch, 1 arthrobranch and 2 podobranchs. Coxa without setae, small distal ventral spine present, basis delimited by small exopod bud and not articulated; endopod with 4 articles, ischium-merus (undifferentiated), carpus, propodus and dactylus with 5, 3, 18, 23 setae (several setae missing in Manta\_

L08) respectively. Setae on inner margin longer than outer margin. Exopod absent.

*Pereiopods* (Figs. 4A–E, 5G): P1–4 biramous. Coxa without setae, small distal ventral spine present; basis delimited by distal spine with 4, 5, 5, 7 setae respectively. Endopod with 4 articles, ischium-merus undifferentiated with 2 distal spines (or 3 in P4) and 0, 5, 7, 12 setae, carpus with 1 distal spine and 5, 5, 4, 4 setae, propodus with 70, 75, 30 and 10 small setae scattered over the surface, dactylus with 7, 6, 2, 2 setae respectively. Exopods with 17, 16, 16 and 16 annulations respectively. P5 uniramous. Coxa without setae, small distal ventral spine present; basis not differentiated, delimited by 1 seta; endopod with 4 articles, ischium-merus undifferentiated with distal seta, carpus with 1 distal setae propodus and dactylus without setae.

*Gills* (Fig. 4A, F): Gill buds present. P1 with 1 pleurobranch, 1 arthrobranch and 2 podobranchs. P2–P4 with 2 pleurobranchs, 1 arthrobranch, 2 podobranchs. P5 with 1 pleurobranch.

*Thorax* (Fig. 4A, F): Without dorsal thoracic spines.

*Pleon* (Figs. 4A, 5G): Pleopod 1 absent. Pleopods 2–5 and uropods biramous and well-developed. Small setae along inner margin of uropods.

*Telson* (Figs. 4A, 5G): 3 paired dorsal setae (not appreciated in Manta\_L08). Two short terminal processes with one seta in outer margin. Setae along margin.

### Morphotype B – *Acantharctus ornatus* (Holthuis, 1960)

Stage VIII (Subfinal)  
(Figs. 6–7)

*Material examined:* Manta\_L30; Manta\_L31; Ring\_L08.

*Morphometrics:* N = 5; BL = 9.06–11.88 mm; CL = 5.89–7.88 mm; CW = 6.15–8.25 mm; TL = 2.83–3.97 mm; TW = 2.97–3.84 mm; PL = 1.42–2.10 mm; PW = 1.43–2.17 mm; BL/CW = 1.4–1.5; CW/TW = 1.9–2.6; ES/A2 ≥ 0.9.

*Cephalic shield* (Fig. 6A): Rounded shape (CL/CW = 1.0).

*Eyestalk* (Figs. 6A, 7A): As long as antenna (ES/A2 = 1).

*Antennule* (Figs. 6A, 7A): Longer than antenna; 3-articled peduncle, articles with 1 seta each one. Primary flagellum with 11 rows of sensory setae. Accessory flagellum not articulated, with 1 proximal and 2 distal setae.

*Antenna* (Figs. 6A, 7A): Uniramous and not articulated; shorter than antennule. Endopod slender

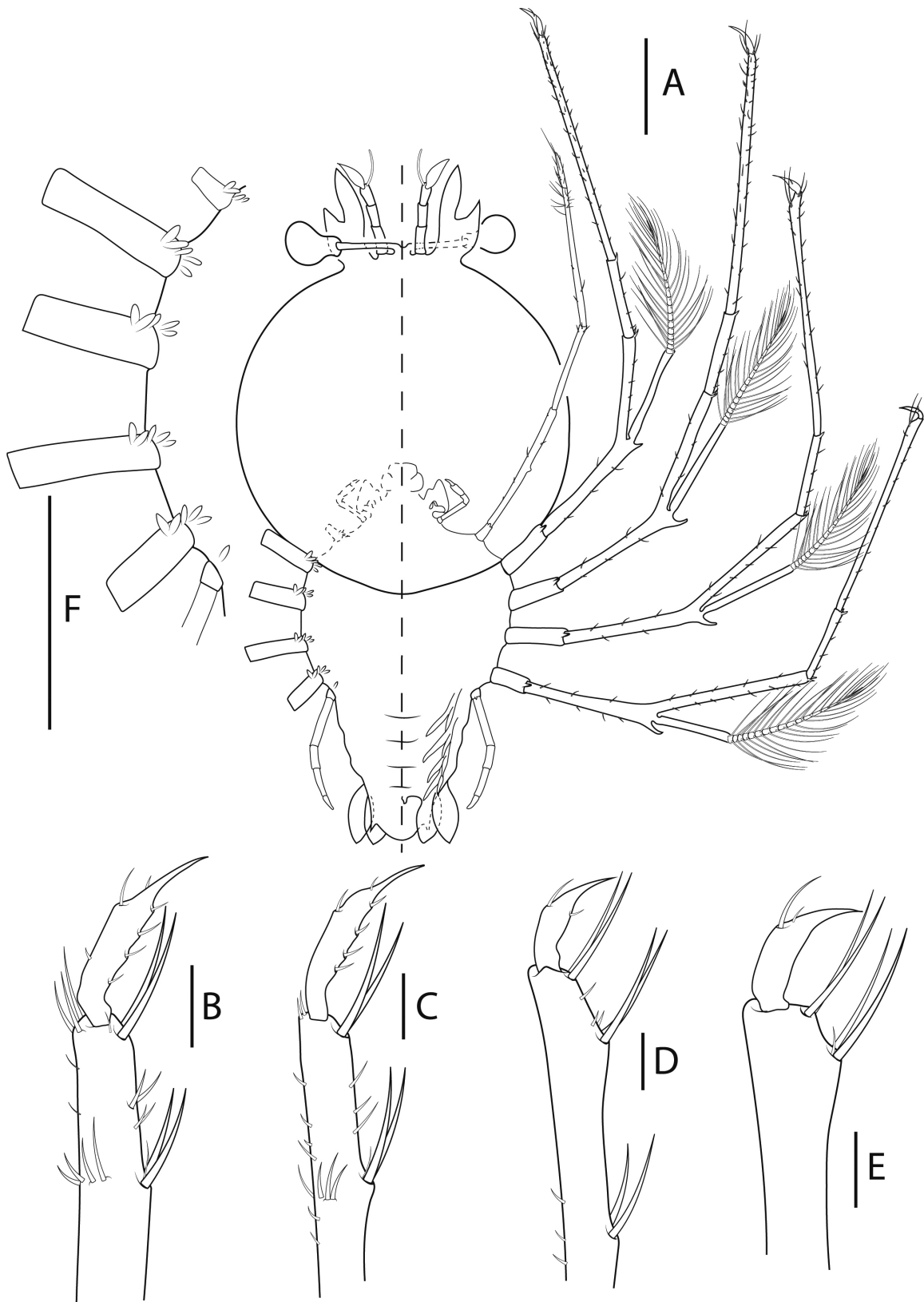


**Fig. 4.** *Biarctus pumilus* (Nobili, 1906), phyllosoma stage IX (Final) (Manta\_L39). A, ventral (right) and dorsal (left) view; B, dactylus of first pereopod; C, dactylus of second pereopod; D, dactylus of third pereopod; E, dactylus of fourth pereopod; F, thorax. Scale bars: A and F = 2 mm; B–E = 200  $\mu$ m.

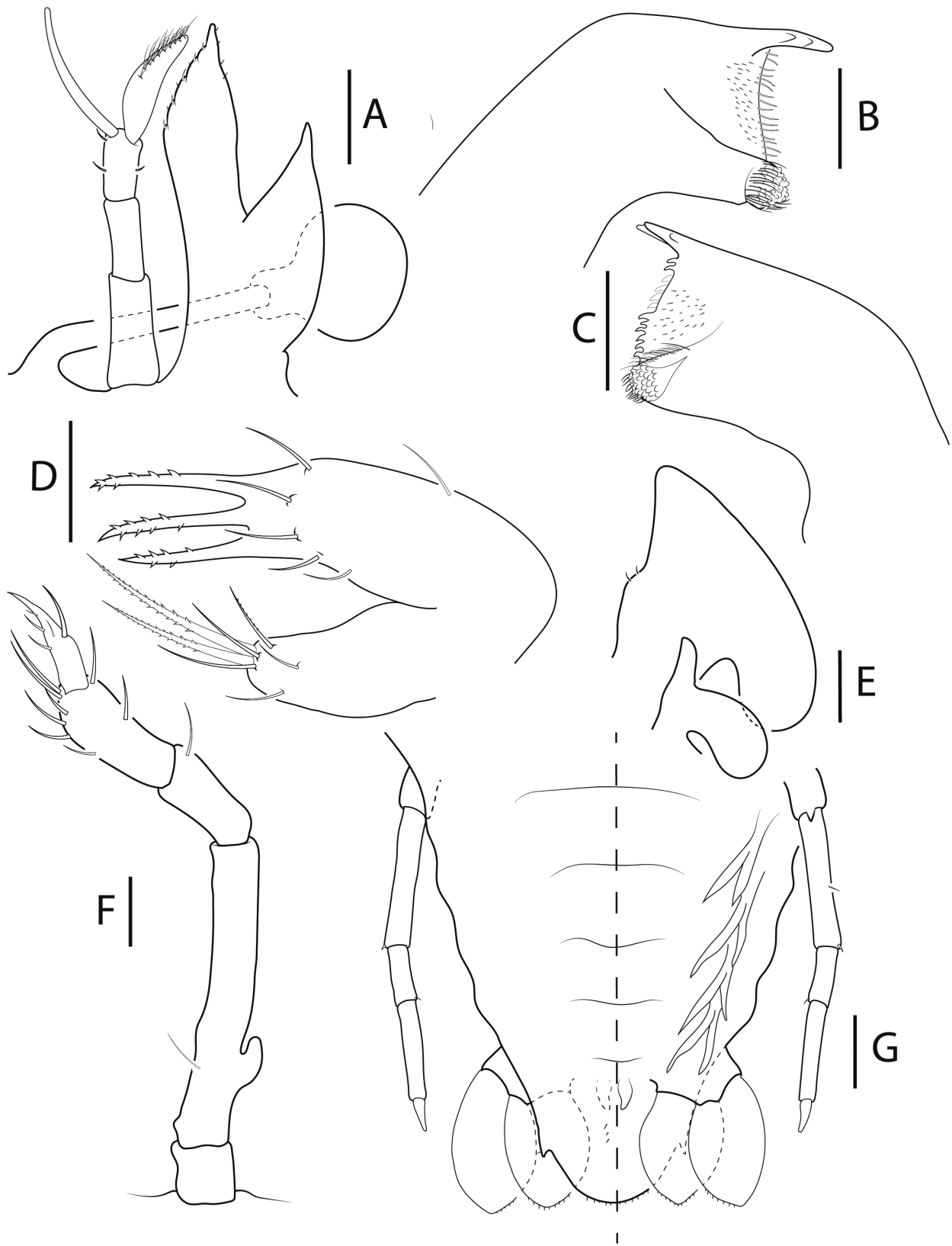


**Fig. 5.** *Biarctus pumilus* (Nobili, 1906), phyllosoma stage IX (Final) (Manta\_L39). A, stalked eye, antennule and antenna; B, C, left and right mandibles (ventral view); D, maxillule; E, maxilla and first maxilliped; F, second maxilliped; G, pleon, fifth pereopod, pleopods 2–5 and uropods, ventral (right) and dorsal (left) view. Scale bars: A = 500  $\mu$ m, B–D = 100  $\mu$ m; E–G = 200  $\mu$ m.

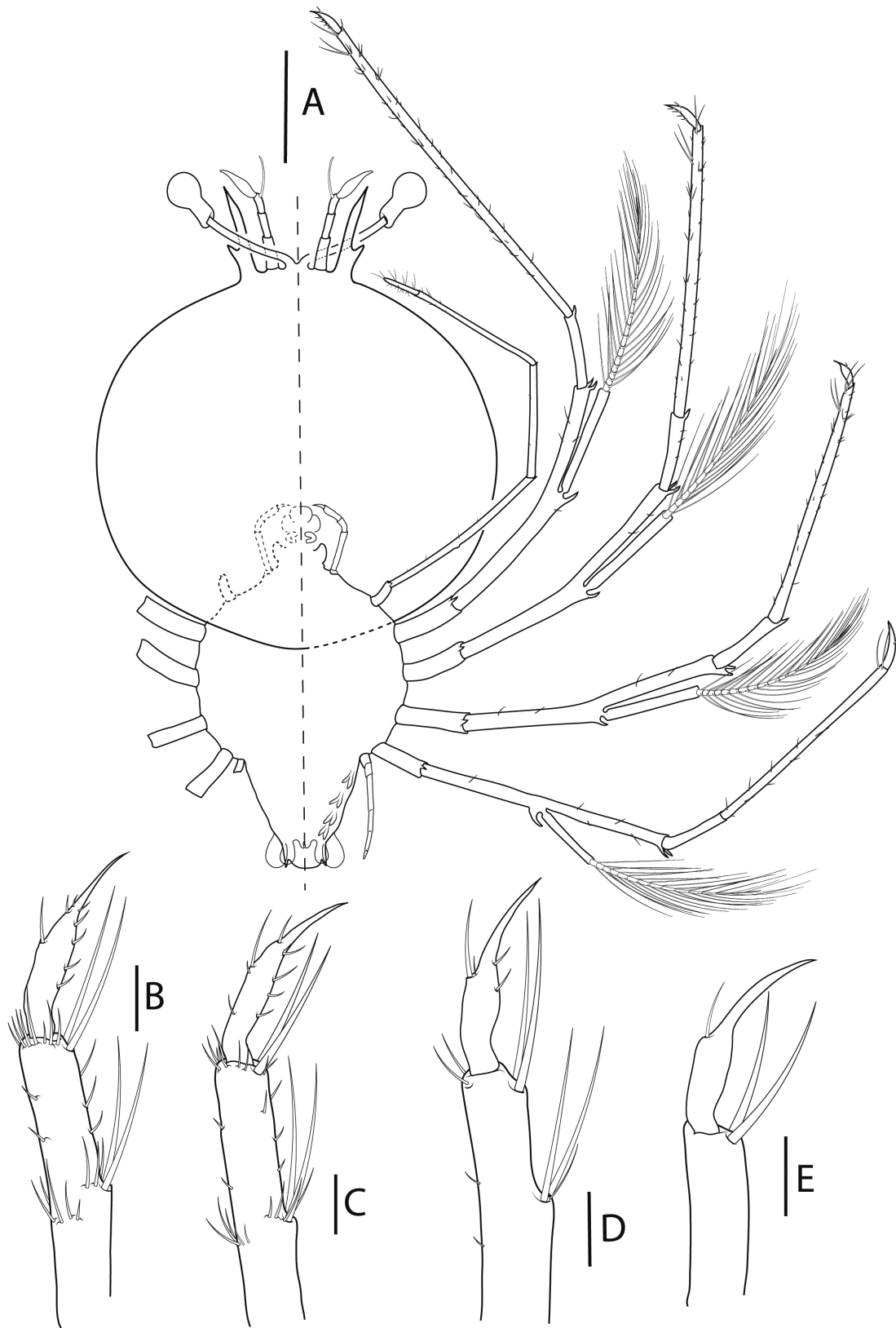


**Fig. 6.** *Acantharctus ornatus* (Holthuis, 1960), phyllosoma stage VIII (subfinal). A, ventral (right) and dorsal (left) view (Ring\_L08); B, dactylus of first pereopod (Manta\_L31); C, dactylus of second pereopod (Manta\_L301); D, dactylus of third pereopod (Manta\_L31); E, dactylus of fourth pereopod (Ring\_L08). Scale bars: A = 2 mm; B–E = 200  $\mu$ m.

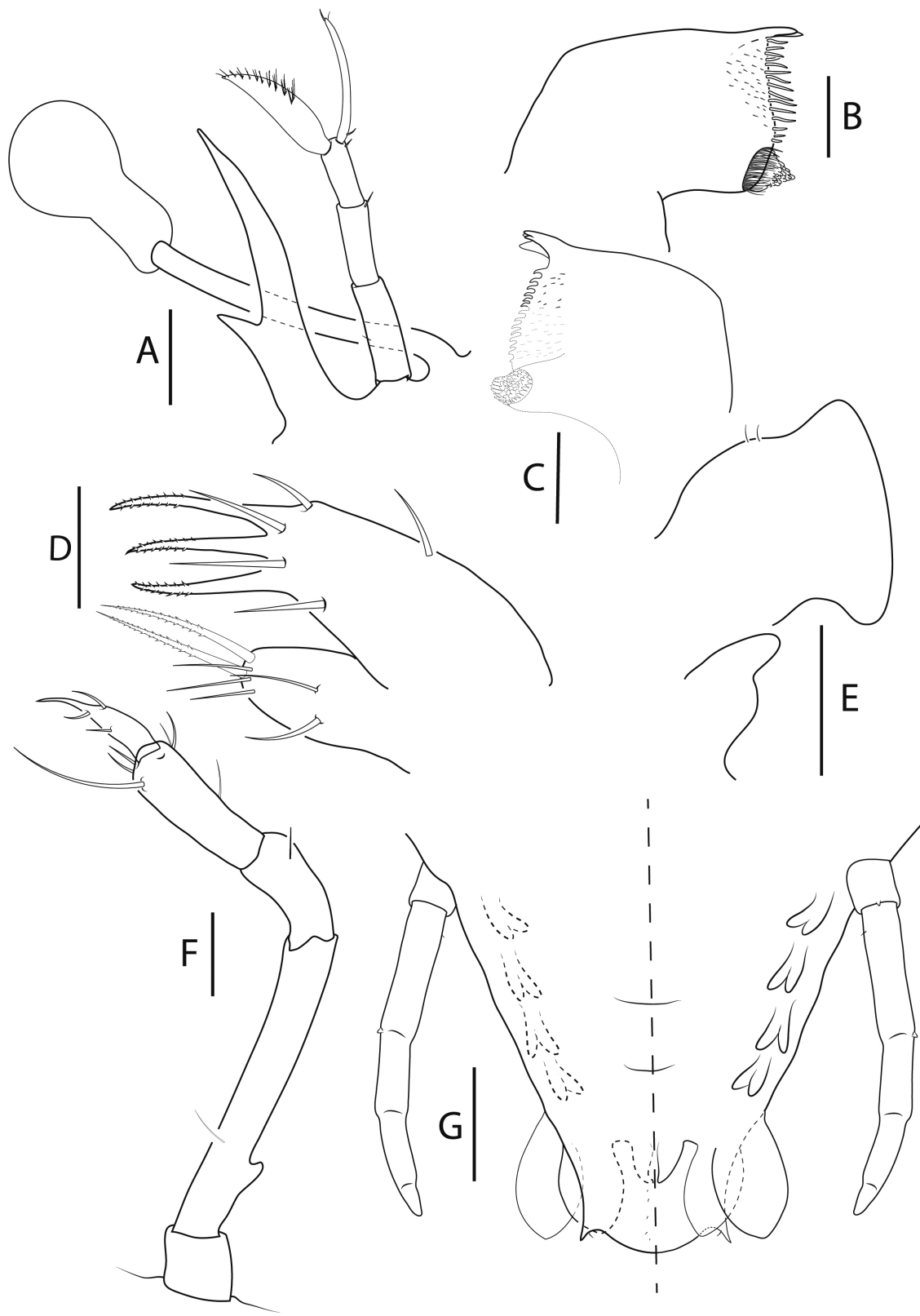


**Fig. 7.** *Acantharctus ornatus* (Holthuis, 1960), phyllosoma stage VIII (Subfinal). A, stalked eye, antennule and antenna (Ring\_L08); B, C, left (Ring\_L08) and right (Manta\_L30) mandibles (ventral view); D, maxillule; E, maxilla and first maxilliped (Ring\_L08); F, second maxilliped (Ring\_L08); G, fifth pereopod, pleopods 2–5 and uropods (ventral view) (Ring\_L08). Scale bars: A and G = 500  $\mu$ m; B–D = 100  $\mu$ m; E and F = 200  $\mu$ m.

with a small medio-lateral expansion. Exopod absent.

*Mandibles* (Fig. 7B–C): Incisor process in left mandible with 2 teeth (probably 2 teeth missing). Right mandible with more curved teeth (damaged, teeth present in dashed line). Palp absent.

*Maxillule* (Fig. 7D): Coxal endite with 7 setae, 2 plumidenticulate; basial endite with 8 setae, 3 serrated, long and strong.

*Maxilla* (Fig. 7E): Uniramous and not articulated. Endites and endopod not differentiated with 2 setae on superior margin; exopod (scaphognathite) present, slightly developed and rectangular, without marginal setae.

*First maxilliped* (Fig. 7E): Uniramous. Coxal and basial endites and endopod undifferentiated. Exopod absent.

*Second maxilliped* (Figs. 6A, 7F): Biramous. Coxa differentiated; basis delimited by 1 seta and exopod bud (missing in Ring\_L08); endopod 4-article, ischium-merus (undifferentiated), carpus, propodus, dactylus with 0, 1, 7 (one missing) and 3 setae respectively. Exopod (bud) present.

*Third maxilliped* (Fig. 6A): Uniramous. Coxa with 1 minute ventral distal spine; basis delimited by small exopod bud; endopod with 4 articles, ischium-merus (undifferentiated), carpus, propodus and dactylus with 4–6, 2, 19 (2 distal serrated) and ~30 setae, respectively. Setae on inner margin longer than outer margin.

*Pereiopods* (Figs. 6A–E, 7G): P1–4 biramous. Coxa without setae, small distal ventral spine present; basis delimited by distal spine; endopod 4-articled, ischium-merus undifferentiated with 2 distal spines and 3, 2, 2, 4 setae, carpus with 1 distal spine, propodus with 66, 74, 44 and 11 small setae scattered over article surface, dactylus with 8, 8, 4, 1 setae respectively. Exopod with 16–18, 15–16, 14, 12–15 annulations respectively. P5 uniramous. Coxa with small ventral distal spine; endopod 2-articled, ischium-merus undifferentiated with 1 distal spine, proximal articles incomplete.

*Thorax* (Fig. 6A): Without dorsal thoracic spines.

*Pleon* (Figs. 6A, 7G): Pleopod 1 absent, pleopods 2–5 and uropods biramous.

*Telson* (Figs. 6A, 7G): Margin distinctly more convex, 5–6 pairs of dorsal setae. Two processes with one inner seta each one.

#### Stage IX (Final) (Figs. 8–9)

*Material examined*: Manta\_L33; Manta\_L62; Manta\_L65; Manta\_L70; Manta\_L73.

*Morphometrics*: N = 16; BL = 13.87–17.83 mm; CL = 8.22–10.35 mm; CW = 8.19–10.22 mm;

TL = 3.59–4.68 mm; TW = 4.53–5.87 mm; PL = 3.54–4.57 mm; PW = 3.10–3.96 mm; BL/CW = 1.6–1.7; CW/TW = 1.7–1.9; ES/A2  $\geq$  0.8.

*Cephalic shield* (Fig. 8A): Unchanged.

*Eyestalk* (Figs. 8A, 9A): Longer than antenna (ES/A2)  $\geq$  1.0.

*Antennule* (Figs. 8A, 9A): Slightly longer than antenna. Second article with 2 setae, 1 medial and 1 distal. Primary flagellum with 12–13 rows of setae. Otherwise, unchanged.

*Antenna* (Figs. 8A, 9A): Uniramous and not articulated; slightly shorter than antennule. Endopod external medio-lateral margin expanded and lobated; distal margin lobated with setae. Exopod absent.

*Mandibles* (Fig. 9B–C): Both mandibles with more teeth than previous stage. Otherwise unchanged.

*Maxillule* (Fig. 9D): Basial endite with 9 setae. Otherwise unchanged.

*Maxilla* (Figs. 8A, 9E): Uniramous. Endites and endopod undifferentiated with 2–3 setae on superior margin of lateral process; exopod (scaphognathite) more flattened and expanded. Otherwise unchanged.

*First maxilliped* (Figs. 8A, 9E): More developed. Endopod elongated. Otherwise unchanged.

*Second maxilliped* (Figs. 8A, 9F): Endopod with 4 articles, ischium-merus (undifferentiated), carpus, propodus, dactylus with 0, 1, 9 and 4 setae respectively. Otherwise unchanged.

*Third maxilliped* (Fig. 8A): Gills buds present; 1 pleurobranch, 1 arthrobranch and 2 podobranchs. More densely setose than previous stage. Basis delimited by small exopod bud; endopod with 4 articles, ischium-merus (undifferentiated), carpus, propodus and dactylus with 4–10, 4–8, 50 (2 distally serrated) and ~100 setae respectively. Otherwise unchanged.

*Pereiopods* (Figs. 8A–E, 9G): P1–4 biramous. Propodus with 80–90, 80–90, 40 and 10–20 small setae scattered over the surface, dactylus with 7–8, 6, 4, 1 setae respectively. Exopods with 18–19, 18, 16–18 and 15–16 annulations respectively. P5 uniramous. Coxa with dorsal small setae; basis not differentiated; endopod with 4 articles, ischium-merus undifferentiated with distal seta, carpus propodus and dactylus without setae.

*Gills* (Fig. 8A, F): Gill buds present. P1 with 1 pleurobranch, 1 arthrobranch and 2 podobranchs. P2–P4 with 2 pleurobranches, 1 arthrobranch, 2 podobranchs. P5 with 1 pleurobranch.

*Thorax* (Fig. 8A, F): Unchanged.

*Pleon* (Figs. 8A, 9G): Pleopods and uropods well-developed. Otherwise unchanged.

*Telson* (Figs. 8A, 9G): 4–5 paired dorsal setae. Two short terminal processes.

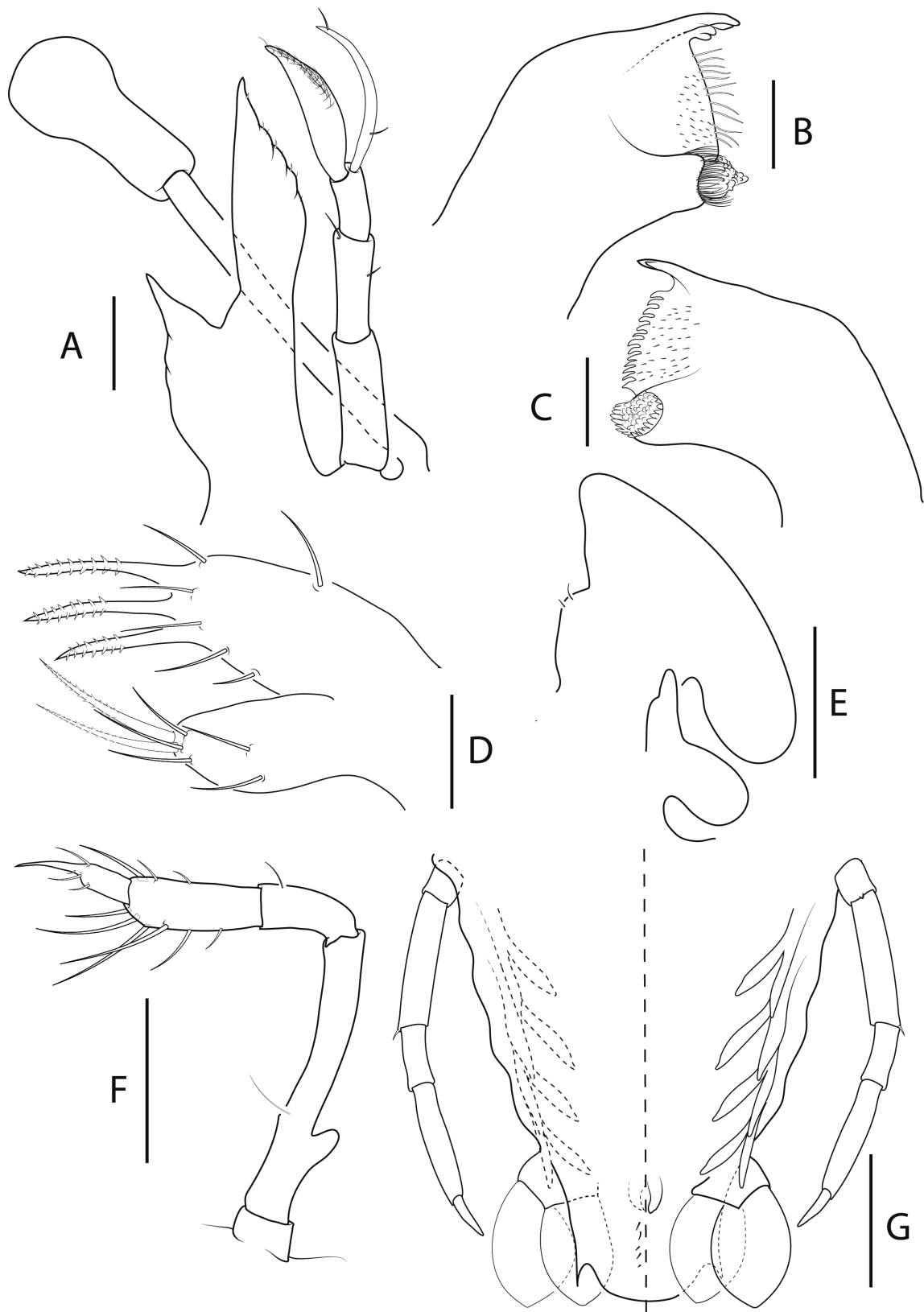


**Fig. 8.** *Acantharctus ornatus* (Holthuis, 1960), phyllosoma stage IX (Final). A, ventral (right) and dorsal (left) view (Manta\_L73); B, dactylus of first pereiopod (Manta\_L70); C, dactylus of second pereiopod (Manta\_L73); D, dactylus of third pereiopod (Manta\_L62); E, dactylus of fourth pereiopod (Manta\_L62); F, thorax (Manta\_L73); G, detail of subexopodal seta (Manta\_L73). Scale bars: A and F–G = 2 mm; B–E = 200  $\mu$ m.

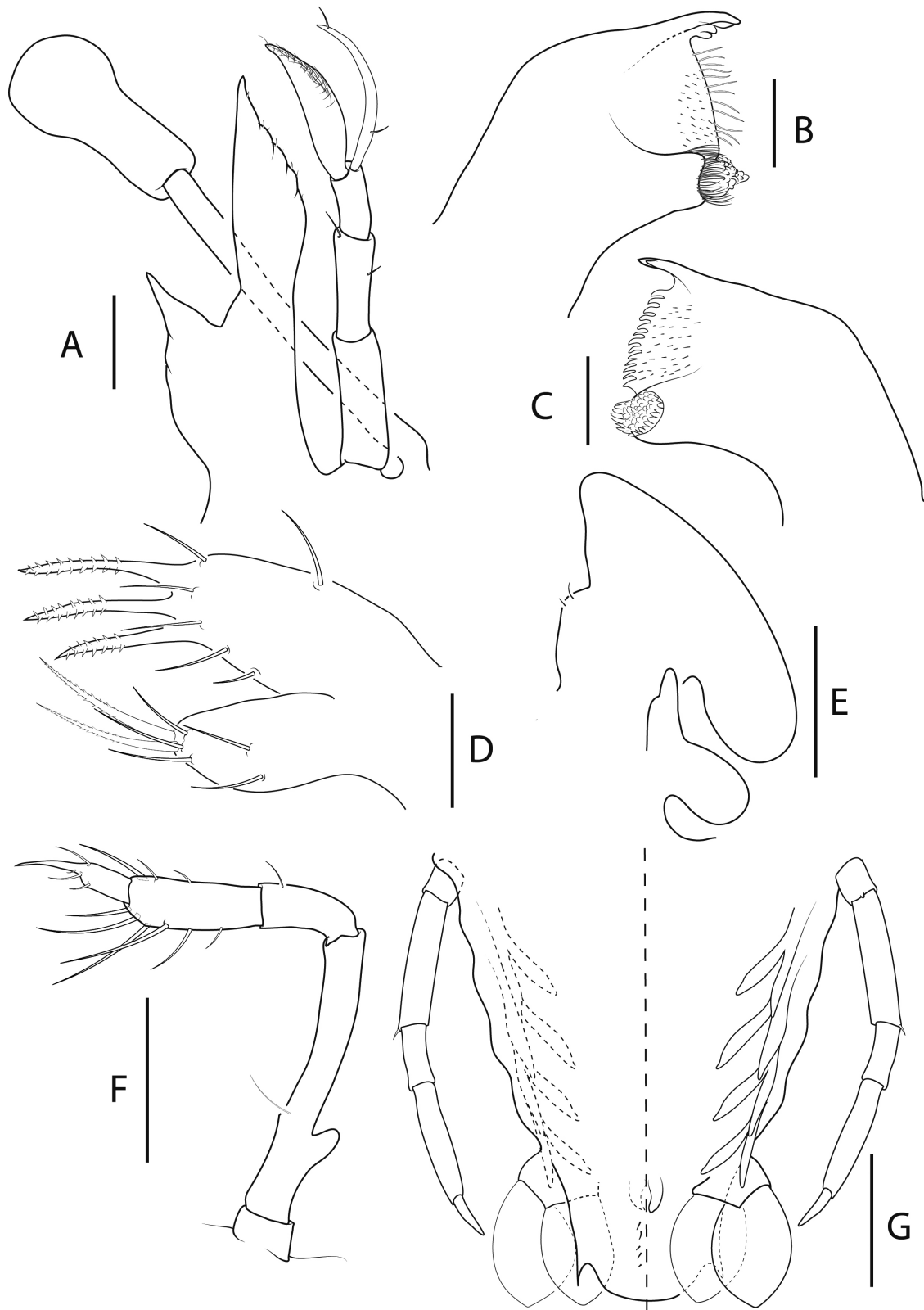


**Fig. 9.** *Acantharctus ornatus* (Holthuis, 1960), phyllosoma stage IX (Final). A, stalked eye, antennule and antenna (Manta\_L73); B, C, left (Manta\_L62) and right (Manta\_L65) mandibles (ventral view); D, maxillule (Manta\_L43); E, maxilla and first maxilliped (Manta\_L62); F, second maxilliped (Manta\_L73); G, pleon, fifth pereiopod and pleopods 2–5 and uropods (ventral view) (Manta\_L73). Scale bars: A and G = 500  $\mu$ m; B–D = 100  $\mu$ m; E–F = 200  $\mu$ m.

### Key of final stage phyllosomas for SW Indian Ocean Scyllaridae genera (excl. *Scammartus* Holthuis, 2002)

- 1a. Large larvae (BL > 30 mm); P3 dactyl long; posterior margin of thorax concave ..... 2
- 1b. Smaller larvae (BL < 30 mm); dactyls of similar length; posterior margin of thorax straight ..... 3
- 2a. (1a) ES/A2 > 1.5×; dorsal spines on pleonites 4 and 5 .....  
..... *Scyllarides*  
Gill, 1898 (Robertson 1969; Johnson 1977; Palero et al. 2016)
- 2b. (1a) ES/A2 < 1.5×; Pleon well-developed, without dorsal spines .....  
..... *Parribacus* Dana, 1852 (Palero et al. 2014)
- 3a. (1b) Cephalon margin reaching P3; P5 exopod plumose .....  
..... *Ibacus* Leach,  
1815 (Atkinson and Boustead 1982; Marinovic et al. 1994)
- 3b. (1b) Cephalon margin not exceeding P2; P5 without exopod .... 4
- 4a. (3b) Pleopods uniramous; P5 longer than pleon and densely setose .....  
..... *Thenus* Leach, 1816 (Barnett et al. 1984)
- 4b. (3b) Pleopods biramous; P5 shorter than pleon and smooth or with few setae ..... 5
- 5a. Cephalon narrow (CW/TW ≤ 1.5); pleon straight .....  
..... *Petrartus* Holthuis, 2002 (Kumar et al. 2009; Wakabayashi et al. 2020)
- 5b. Cephalon wider (CW/TW ≥ 1.6); pleon conic, wider at the base ..... 6
- 6a. (5b) Dorsal thoracic spines in P2–P4 or P3–P4; Crp/Prd ≥ 0.9; P5 3-articled ..... 7
- 6b. (5b) Dorsal thoracic spines in P1–P4 or absent; Crp/Prd ≤ 0.8; P5 4 or 5-articled ..... 8
- 7a. (6a) Cephalon kidney-shaped or pentagonal and covering P2; BL/CW = 1.0–1.4 .....  
..... *Chelarctus* Holthuis, 2002 (Genis-Armero et al. 2022)
- 7b. (6a) Cephalon round and narrower, and covers P1; BL/CW = 1.5–1.8 .....  
..... *Galearctus* Holthuis, 2002 (Higa et al. 2005)
- 8a. (6b) Dorsal thoracic spines in P1–P4; telson spines exceed pleopod I .....  
..... *Crenarctus* Holthuis, 2002 (Genis-Armero et al. 2022)
- 8b. (6b) Dorsal thoracic spines absent; telson spines do not exceed pleopods ..... 9
- 9a. (8b) Cephalon trapezoidal; pleopods sharply pointed; large coxal spines on pereopods .....  
..... *Eduarctus* Holthuis, 2002 (Wakabayashi et al. 2017)
- 9b. (8b) Cephalon rounded or oval; pleopods leaf-shaped; minute coxal spines on pereopods ..... 10
- 10a. (9b) Eyestalk short (ES/A2 ≤ 0.5); cephalon shield oval and narrow (CW/TW = 1.6); uropods leaf-shaped .....  
..... *Biarctus* Holthuis, 2002 (Present study)
- 10b. (9b) Eyestalk longer (ES/A2 ≥ 0.9); cephalon shield round and wider (CW/TW ≥ 1.7); uropod rounded .....  
..... *Acantharctus* Holthuis, 2002 (Present study)

\*Crp/prd = third maxilliped carpus length/propodus length ratio.

## DISCUSSION

New molecular and morphological analyses of phyllosomas collected during the RV *Dr Fridtjof Nansen* survey in 2018 have allowed the assignment of two phyllosoma morphotypes to *Biarctus* and *Acantharctus*. Previous DNA barcoding analyses of phyllosoma larvae of eastern South Africa (Govender et al. 2019)

had incorrectly identified specimens corresponding to our morphotype A as *A. ornatus* and those similar to our morphotype B as *P. rugosus*, based on reference sequences on BOLD and GenBank at the time. A morphological revision of *A. ornatus* type material revealed that the putative *A. ornatus* from GenBank (WAM C27134) was misidentified, and it likely belongs to *Biarctus dubius* instead. The molecular results of this study also indicate that morphotype A should be assigned to *Biarctus*, together with the undescribed phyllosoma (GenBank accession: MK113916) in Govender et al. (2019). We suggest that morphotype A belongs to *B. pumilus* (Nobili, 1906) given that it is the only known species from the Western Indian Ocean, originally described from the Red Sea (Nobili 1906).

DNA sequences from morphotype B larvae significantly clustered with sequences of *A. posteli*, and they must correspond to *A. ornatus*, the only species of the genus known from SE Africa (Berry 1974; Holthuis 2002; Genis-Armero et al. 2020). Although no DNA sequence data could be obtained from *A. ornatus* adults, the new evidence allows for assignment of larval morphotypes A and B at least to genus level, providing further insights on the identity of phyllosomas from the historical literature.

The phyllosomas assigned to *P. rugosus* and *S. ornatus* by Berry (1974), named as sp. A and sp. C, correspond in fact to *A. ornatus* and *B. pumilus*, respectively. Moreover, the relative abundances of both species in Berry (1974) were consistent with our observations. Unassigned *Biarctus* phyllosoma were described as *Scyllarus* sp. C from Australian Pacific waters by Barnett (1989) and as *Scyllarus* sp. F and H from the eastern Indian Ocean by McWilliam et al. (1995). Those larvae could well belong to *B. dubius* since they share key traits with *Biarctus* phyllosomas described here, such as a particularly short eyestalk, wide lateral antennal process, and leaf-shaped uropods. As for morphotype B, it is closest in morphology to *Scyllarus* larva “type A-B” described from the Mauritanian Coast by Maigret (1975 1978) and tentatively assigned to *A. posteli*. Indeed, *A. posteli* and morphotype B (*A. ornatus*) phyllosomas share many morphological traits, such as the round cephalic shield, long eyestalks, 5-articled P5 and telson spines not exceeding the rounded uropods. Finally, *Acantharctus* phyllosomas are distinct from the Pacific Ocean phyllosoma assigned to *A. delfini* (Johnson 1971; Baez 1973), providing further morphological evidence for the polyphyletic origin of the genus sensu Holthuis (2002), as supported by adult morphology and molecular results (Bracken-Grissom et al. 2014; Genis-Armero et al. 2020).

Surprisingly, no adult *A. ornatus*, by far the most abundant species in historical and recent phyllosoma

collections, have been reported from South African waters (pers. obs. JCG). Alternative hypotheses are that adults inhabit nearby seafloor habitats that have not previously been sampled, or that phyllosomas that originate from upstream adult populations in the SW Indian Ocean are advected southwards along the African coast by predominant currents. The presence of tropical Western Indian Ocean decapod species in zooplankton collected off eastern South Africa (Govender et al. 2022a) strongly supports the advection hypothesis. Nevertheless, similar cases have been reported in the Mediterranean Sea, where the most abundant larvae belong to *S. pygmaeus* Bate, 1888, confused with juveniles of *S. arctus* (Linnaeus, 1758), and unreported in the area until the 1960s (Palero et al. 2008 2011).

The relative abundance and distribution of *Biarctus* and *Acantharctus* phyllosomas are potentially affected by reproductive cycles and larval transport by water movements (Phillips et al. 2006; Singh et al. 2018 2019). Nearly all phyllosomas collected during the RV *Dr Fridtjof Nansen* survey originated from the northern KZN Bight, similar to the results of Berry (1974). Subsequent sampling also identified phyllosoma concentrations over the southern KZN Bight (pers. obs. JCG). The interaction of the nearshore Agulhas Current edge and topography of the KZN Bight is known to produce eddies and counter currents (Roberts et al. 2016), which retain drifting larvae in a sheltered nursery area (Hutchings et al. 2002; Govender et al. 2022b). Even so, offshore larval development is well described in Palinuridae (Griffin et al. 2001; Jeffs et al. 2005) and some Scyllaridae (Booth et al. 2005; Genis-Armero et al. 2019). Therefore, the alternative explanation that higher phyllosoma concentrations over the KZN Bight is related to shelf-edge upwelling cells (Meyer et al. 2002; Omarjee 2012) cannot be discarded. Available samples were restricted to surface waters, and given that scyllarid phyllosomas undertake daily vertical migrations (Griffin et al. 2001; Minami et al. 2001; Booth et al. 2005) and have been reported below 200 m depth (Palero et al. 2008 2011; Genis-Armero et al. 2017), it is not unlikely that they also occur in deeper layers of the KZN Bight and beyond.

## CONCLUSIONS

An integrated taxonomy approach coupled with a revision of misidentified museum specimens allowed the assignment of two phyllosoma morphotypes to *Biarctus* and *Acantharctus*, genera for which the larval morphology was unknown or incorrectly attributed until now. Scyllarid biodiversity in eastern South Africa is potentially underestimated, with phyllosoma

larvae from the Western Indian Ocean species also present in the zooplankton. Sampling of deeper water layers is required to collect and describe phyllosomas in all developmental stages, thus allowing for detailed biodiversity and ecological research. Improving the Scyllaridae reference sequences in BOLD and GenBank databases is a key step in future species-level identification of phyllosomas.

**Acknowledgments:** Thanks are due to Kevin Webb, science photographer at the Natural History Museum (London), for helping us with the photographs of *A. ornatus* syntypes. FP acknowledges “the project “CIDEAGENT/2019/028 - BIodiversity PATterns of Crustacea from Karstic Systems (BIOPACKS): molecular, morphological, and functional “adaptations” funded by the Conselleria d’Innovació, Universitats, Ciència i Societat Digital. The EAF-Nansen Programme of the FAO is thanked for access to phyllosoma samples collected during a survey off eastern South Africa.

**Authors’ contributions:** JG and SS collected and photographed the specimens. RGA carried out drawings and, together with FP and PC, completed the descriptions. LC was crucial in obtaining sequence data for the MNHN type material. FP completed the molecular analyses and, together with RGA, prepared a manuscript draft. All authors contributed to the final version of the text.

**Competing interests:** The authors declare that they have no competing interests.

**Availability of data and materials:** DNA sequences generated in the study have been deposited in GeneBank.

**Consent for publication:** All the authors consent to the publication of this manuscript.

**Ethics approval consent to participate:** This research followed the standard guidelines for sampling marine invertebrates and does not include any research on humans.

## REFERENCES

- Atkinson JM, Boustead NC. 1982. The complete larval development of the scyllarid lobster *Ibacus alticrenatus* Bate, 1888 in New Zealand Waters. *Crustaceana* **42**:275–287. doi:10.1163/156854082X00344.
- Baez P. 1973. Larvas phyllosoma del Pacífico Sur Oriental (Crustacea, Macrura, Scyllaridea). *Rev Biol Mar* **15**:115–130.
- Barnett BM. 1989. Final-stage phyllosoma larvae of Scyllarus species

- (Crustacea: Decapoda: Scyllaridae) from shelf waters of the great barrier reef. *Invert Syst* **3**(2):123–134.
- Barnett BM, Hartwick RF, Milward NE. 1984. Phyllosoma and nisto stage of the Moreton bay bug, *Thenus orientalis* (Lund) (Crustacea: Decapoda: Scyllaridae), from shelf waters of the great barrier reef. *Mar Freshw Res* **35**:143–152. doi:10.1071/MF9840143.
- Berry PF. 1974. Palinurid and Scyllarid lobster larvae of the Natal coast, South Africa. *Invest Rep Oceanogr Res Inst* **34**:1–44
- Booth JD, Webber WR, Sekiguchi H, Coutures E. 2005. Diverse larval recruitment strategies within the Scyllaridae. *NZ J Mar Freshw Res* **39**:581–592. doi:10.1080/00288330.2005.9517337.
- Boxshall GA. 2004. The evolution of arthropod limbs. *Biol Rev* **79**(2):253–300. doi:10.1017/S1464793103006274.
- Boxshall GA, Danielopol DL, Horne DJ, Smith RJ, Tabacaru I. 2010. A critique of biramous interpretations of the crustacean antennule. *Crustaceana* **83**:153–167. doi:10.1163/001121609X12530988607434.
- Bracken-Grisson HD, Ah Yong ST, Wilkinson RD, Feldmann RM, Schweitzer CE, Breinholt JW, Bendall M, Palero F, Chan TY, Felder DL, Robles R, Chu KH, Tsang LM, Kim D, Martin JW, Crandall KA. 2014. The emergence of lobsters: Phylogenetic relationships, morphological evolution and divergence time comparisons of an ancient group (Decapoda: Achelata, Astacidea, Glypheidea, Polychelida). *Syst Biol* **63**:457–479. doi:10.1093/sysbio/syu008.
- Chan TY. 2019. Updated checklist of the world's marine lobsters. *In: Radhakrishnan EV, Phillips BF, Achamveetil G* (eds) *Lobsters: Biology, Fisheries and Aquaculture*: Springer, Singapore, pp. 35–64.
- Clark PF, Calazans DK, Pohle GW. 1998. Accuracy and standardization of brachyuran larval descriptions. *Invert Reprod Dev* **33**:127–144. doi:10.1080/07924259.1998.9652627.
- Clark PF, Cuesta JA. 2015. Larval systematics of the Brachyura. *In: Castro P, Davie PJP, Guinot D, Schram FR, von Vaupel Klein JC* (eds) *The Crustacea, Treatise on Zoology - Anatomy, Taxonomy, Biology. Decapoda: Brachyura vol. 9 (Part C-II)*. Brill, Leiden, Boston, pp. 981–1048.
- Coleman CO. 2003. “Digital inking”: How to make perfect line drawings on computers. *Org Divers Evol* **3**:303–304. doi:10.1078/1439-6092-00081.
- Coleman CO. 2009. Drawing setae the digital way. *Zoosyst Evol* **85**:305–310. doi:10.1002/zoos.200900008.
- Edgar RC. 2004. MUSCLE: Multiple sequence alignment with high accuracy and high throughput. *Nucleic Acids Res* **32**:1792–1797. doi:10.1093/nar/gkh340.
- Emmerson WD (ed). 2016. A Guide to, and Checklist for, the Decapoda of Namibia, South Africa and Mozambique, Vol. 1–3. Cambridge Scholars Publishing.
- Genis-Armero R, Błażewicz M, Clark PF, Palero F. 2022. *Chelarctus* and *Crenarctus* (Crustacea: Scyllaridae) from Coral Sea waters, with molecular identification of their larvae. *Eur Zool J* **89**:446–466. doi:10.1080/24750263.2022.2036256.
- Genis-Armero R, González-Gordillo JI, Cuesta JA, Capaccioni-Azzati R, Palero F. 2020. Revision of the West African species of *Scyllarus* Fabricius, 1775 (Decapoda: Achelata: Scyllaridae), with the description of three phyllosoma stages of *S. caparti* Holthuis, 1952 and an updated identification key. *J Crust Biol* **40**:412–424. doi:10.1093/jcobiol/ruaa025.
- Genis-Armero R, Guerao G, Abelló P, González-Gordillo JI, Cuesta JA, Corbari L, Clark PF, Capaccioni-Azzati R, Palero F. 2017. Possible amphi-atlantic dispersal of *Scyllarus* lobsters (Crustacea: Scyllaridae): Molecular and larval evidence. *Zootaxa* **4306**:325–338. doi:10.11646/zootaxa.4306.3.2.
- Genis-Armero R, Landeira J, Capaccioni-Azzati R, Palero F. 2019. Updated distribution and first description of *Scyllarus subarctus* (Crustacea: Scyllaridae) decapodid stage. *J Mar Biol Assoc UK* **99**:1181–1188. doi:10.1017/S0025315419000067.
- Govender A, Groeneveld J, Singh S, Willows-Munro S. 2019. The design and testing of mini-barcode markers in marine lobsters. *PLoS ONE* **14**:1–11. doi:10.1371/journal.pone.0210492.
- Govender A, Singh SP, Groeneveld JC, Willows-Munro S. 2022a. Metabarcoding of zooplankton confirms southwards dispersal of decapod crustacean species in the Western Indian Ocean. *Afri J Mar Sci* **44**:279–289. doi:10.2989/1814232X.2022.2108144.
- Govender A, Singh S, Groeneveld J, Pillay S, Willows-Munro S. 2022b. Metabarcoding analysis of marine zooplankton confirms the ecological role of a sheltered bight along an exposed continental shelf. *Mol Ecol* **00**:1–13. doi:10.1111/mec.16567.
- Griffin DA, Wilkin JL, Chubb CF, Pearce AF, Caputi N. 2001. Ocean currents and the larval phase of Australian western rock lobster, *Panulirus cygnus*. *Mar Freshw Res* **52**:1187–99. doi:10.1071/mf01181\_co.
- Guindon S, Dufayard JF, Lefort V, Anisimova M, Hordijk W, Gascuel O. 2010. New algorithms and methods to estimate maximum-likelihood phylogenies: Assessing the performance of PhyML 3.0. *Syst Biol* **59**:307–321. doi:10.1093/sysbio/syq010.
- Hall T. 1999. Symposium on RNA Biology. III. RNA, Tool and Target. Research Triangle Park, North Carolina, USA. October 15–17, 1999. *Proc Nucleic Acids Symp Ser* **41**:1–218.
- Hidaka C, Yang CH, Wakabayashi K. 2022. Finding the missing puzzle piece of the nisto stage in the larval cycle of the slipper lobster *Scyllarides squammosus*: a molecular and morphological approach. *Zool Stud* **61**:73. doi:10.6620/ZS.2022.61-73.
- Higa T, Fujita Y, Shigemitsu S. 2005. Complete larval development of a scyllarine lobster, *Galearctus kitanovirus* (Harada, 1962) (Decapoda: Scyllaridae: Scyllarinae), reared under laboratory conditions. *Crust Res* **34**:1–26. doi:10.18353/crustacea.34.0\_1.
- Higa T, Shokita S. 2004. Late-stage phyllosoma larvae and metamorphosis of a scyllarid lobster, *Chelarctus cultrifer* (Crustacea: Decapoda: Scyllaridae), from the Northwestern Pacific. *Species Divers* **9**:221–249. doi:10.12782/specdiv.9.221.
- Holthuis LB. 2002. The Indo-Pacific scyllarine lobsters (Crustacea, Decapoda, Scyllaridae). *Zoosystema* **24**:499–683.
- Hutchings L, Beckley LE, Griffiths MH, Roberts MJ, Sundby S, van der Lingen C. 2002. Spawning on the edge: spawning grounds and nursery areas around the southern African coastline. *Mar Freshw Res* **53**:307–318. doi:10.1071/MF01147.
- Inoue N, Sekiguchi H. 2006. Descriptions of phyllosoma larvae of *Scyllarus bicuspidatus* and *S. cultrifer* (Decapoda, Scyllaridae) collected in Japanese waters. *Plankton Benthos Res* **1**:26–41. doi:10.3800/pbr.1.26.
- Jeffs AG, Montgomery JC, Tindle CT. 2005. How do spiny lobster post-larvae find the coast? *NZ J Mar Freshw Res* **39**:605–617. doi:10.1080/00288330.2005.9517339.
- Johnson MW. 1971. The phyllosoma larva of *Scyllarus delphin* (Bouvier) (Decapoda, Palinuridae). *Crustaceana* **21**:161–164.
- Johnson MW. 1977. On a hitherto unknown phyllosoma larval species of the slipper lobster *Scyllarus* (Decapoda, Scyllaridae) in the Hawaiian Archipelago. *Pac Sci* **31**:187–190.
- Kumar TS, Vijayakumaran M, Murugan TS, Jha DK, Sreeraj G, Muthukumar S. 2009. Captive breeding and larval development of the scyllarine lobster *Petrarctus rugosus*. *NZ J Mar Freshw Res* **43**:101–112. doi:10.1080/00288330909509985.
- Lavalli KL, Spanier E, Goldstein JS. 2019. Scyllarid lobster biology and ecology. *In: Diarte-Plata G, Escamilla-Montes R* (eds) *Crustacea*. IntechOpen, p. 26.
- Lazarus BI. 1967. The occurrence of phyllosomata off the Cape with

- particular reference to *Jasus lalandii*. S Afr Div Sea Fish Invest Rep **63**:1–38.
- Lindley JA, Hernández F, Tejera E, Correia SM. 2004. Phyllosoma larvae (Decapoda: Palinuridea) of the Cape Verde Islands. J Plankton Res **26**:235–240. doi:10.1093/plankt/fbh019.
- Maigret J. 1975. Larves phyllosomes capturées au large du banc d'Arguin. Bull Inst Fond Afr Noire **37**:784–794.
- Maigret J. 1978. Contribution à l'étude des langoustes de la côte occidentale d'Afrique (Crustacés, Décapodes, Palinuridae). Bull Inst Fond l'Afr Noire **40**:36–80.
- Marinovic B, Lemmens JWTJ, Knott B. 1994. Larval development of *Ibacus peronii* Leach (Decapoda: Scyllaridae) under laboratory conditions. J Crust Biol **14**:80–96.
- McWilliam PS. 1995. Evolution in the phyllosoma and puerulus phases of the spiny lobster genus *Panulirus* White. J Crust Biol **15**:542–557.
- McWilliam PS, Phillips BF, Kelly S. 1995. Phyllosoma larvae of *Scyllarus* species (Decapoda, Scyllaridae) from the shelf waters of Australia. Crustaceana **68**:537–656.
- Meyer AA, Lutjeharms JRE, De Villiers S. 2002. The nutrient characteristics of the Natal Bight, South Africa. J Mar Syst **35**:11–37. doi:10.1016/S0924-7963(02)00043-X.
- Michalsen K, Olsen M, Bruck SA, Cervantes D, Alvestad AH, Fennessy S, Green A, MacKay F, Huggett J, Sink K, Tsanwani M, Cedras R, Leslie R, Kunnen T, Holleman W, Sonnenberg W, Everett B. 2018. Survey of the marine fishery resources and ecosystems of Southeast Africa, 19 January – 10 February 2018. Norad-FAO Programme Gcp/Glo/690/Nor, Cruise Reports Dr Fridtjof Nansen, EAF-Nansen/Cr/2018/1.
- Minami H, Inoue N, Sekiguchi H. 2001. Vertical Distributions of Phyllosoma Larvae of Palinurid and Scyllarid Lobsters in the Western North Pacific. J Oceanogr **57**:743–748. doi:10.1023/A:1021244711315.
- Nobili G. 1906. Diagnoses préliminaires de 34 espèces et variétés nouvelles, et de 2 genres nouveaux de Décapodes de la Mer Rouge. Bull Mus Natl Hist Nat **6**:393–411.
- Omarjee A. 2012. Phytoplankton Studies in the KwaZulu-Natal Bight. Dissertation. University of KwaZulu-Natal.
- Palero F, Crandall KA, Abelló P, Macpherson E, Pascual M. 2009a. Phylogenetic relationships between spiny, slipper and coral lobsters (Crustacea, Decapoda, Achelata). Mol Phylogen Evol **50**:152–162. doi:10.1016/j.ympev.2008.10.003.
- Palero F, Genis-Armero R, Hall M, Clark PF. 2016. DNA barcoding the phyllosoma of *Scyllarides squamosus* (H. Milne Edwards, 1837) (Decapoda: Achelata: Scyllaridae). Zootaxa **4139**:481–498. doi:10.11646/zootaxa.4139.4.2.
- Palero F, Guerao G, Abelló P. 2008. Morphology of the final stage phyllosoma larva of *Scyllarus pygmaeus* (Crustacea: Decapoda: Scyllaridae), identified by DNA analysis. J Plankton Res **30**:483–488. doi:10.1093/plankt/fbn012.
- Palero F, Guerao G, Clark PF, Abelló P. 2009b. The true identities of the slipper lobsters *Nisto laevis* and *Nisto asper* (Crustacea: Decapoda: Scyllaridae) verified by DNA analysis. Invert Syst **23**:77–85. doi:10.1071/IS08033.
- Palero F, Guerao G, Clark PF, Abelló P. 2011. *Scyllarus arctus* (Crustacea: Decapoda: Scyllaridae) final stage phyllosoma identified by DNA analysis, with morphological description. J Mar Biol Assoc UK **91**:485–492. doi:10.1017/S0025315410000287.
- Palero F, Guerao G, Hall M, Chan TY, Clark PF. 2014. The 'giant phyllosoma' are larval stages of *Parribacus antarcticus* (Decapoda: Scyllaridae). Invert Syst **28**:258–276. doi:10.1071/IS13037.
- Palero F, Hall S, Clark PF, Johnston D, Mackenzie-Dodds J, Thatje S, Johnston J. 2010. DNA extraction from formalin-fixed tissue: new light from the Deep-Sea. Sci Mar **74**:465–470. doi:10.3989/scimar.2010.74n3465.
- Phillips BF, Booth JD, Cobb JS, Jeffs AG, McWilliam P. 2006. Larval and Postlarval Ecology. In: Phillips B (ed) Lobsters: Biology, Management, Aquaculture and Fisheries. Wiley Online Library, pp. 231–262.
- Roberts MJ, Nieuwenhuys C, Guastella LA. 2016. Circulation of shelf waters in the KwaZulu-Natal Bight, South Africa. Afr J Mar Sci **38**:S7–S21. doi:10.2989/1814232X.2016.1175383.
- Robertson PB. 1969. The early larval development of the scyllarid lobster *Scyllarides aequinoctialis* (Lund) in the laboratory, with a revision of the larval characters of the genus. Deep Res Oceanogr Abstr **16**:557–586. doi:10.1016/0011-7471(69)90059-X.
- Robertson PB. 1971. The larvae and postlarvae of the scyllarid lobster *Scyllarus depressus* (Smith). Bull Mar Sci **21**:841–865.
- Schneider CA, Rasband WS, Eliceiri KW. 2012. NIH Image to ImageJ: 25 years of image analysis. Nat Methods **9**:671–675. doi:10.1038/nmeth.2089.
- Singh SP, Groeneveld JC, Hart-Davis MG, Backeberg BC, Willows-Munro S. 2018. Seascape genetics of the spiny lobster *Panulirus homarus* in the Western Indian Ocean: Understanding how oceanographic features shape the genetic structure of species with high larval dispersal potential. Ecol Evol **8**(23):12221–12237. doi:10.1002/ece3.4684.
- Singh SP, Groeneveld JC, Willows-Munro S. 2019. Between the current and the coast – genetic connectivity in the spiny lobster *Panulirus homarus rubellus*, despite potential barriers to gene flow. Mar Biol **166**(3):1–16. doi:10.1007/s00227-019-3486-4.
- Singh SP, Groeneveld JC, Huggett J, Naidoo D, Cedras R, Willows-Munro S. 2021. Metabarcoding of marine zooplankton in South Africa. Afr J Mar Sci **43**(2):1–13. doi:10.2989/1814232X.2021.1919759.
- Tamura K, Stecher G, Kumar S. 2021. MEGA11: Molecular Evolutionary Genetics Analysis Version 11. Mol Biol Evol **38**:3022–3027. doi:10.1093/MOLBEV/MSAB120.
- Ueda K, Yanagimoto T, Chow S, Kuroki M, Yamakawa T. 2021. Molecular identification of mid to final stage slipper lobster phyllosoma larvae of the genus *Chelarctus* (Crustacea: Decapoda: Scyllaridae) collected in the Pacific with descriptions of their larval morphology. Zool Stud **60**:75. doi:10.6620/ZS.2021.60-75.
- von Bonde W. 1930. Post-brephalus development of some South African Macrura. Rep Fish Mar. Biol Surv Un S. Afri **8**:1–42.
- Wakabayashi K, Sato R, Hirai A, Ishii H, Akiba T, Tanaka Y. 2012. Predation by the phyllosoma larva of *Ibacus novemdentatus* on various kinds of venomous jellyfish. Biol Bull **222**:1–5. doi:10.1086/BBLv222n1p1.
- Wakabayashi K, Yang C-H, Chan T-Y, Phillips BF. 2020. The final phyllosoma, nisto, and first juvenile stages of the slipper lobster *Petarctus brevicornis* (Holthuis, 1946) (Decapoda: Achelata: Scyllaridae). J Crust Biol **40**:237–246. doi:10.1093/jcibi/ruaa013.
- Wakabayashi K, Yang CH, Shy JY, He CH, Chan TY. 2017. Correct identification and redescription of the larval stages and early juveniles of the slipper lobster *Eduarctus martensii* (Pfeffer, 1881) (Decapoda: Scyllaridae). J Crust Biol **37**:204–219. doi:10.1093/jcibi/rux009.
- Yang CH, Bracken-Grissom H, Kim D, Crandall KA, Chan TY. 2012. Phylogenetic relationships, character evolution, and taxonomic implications within the slipper lobsters (Crustacea: Decapoda: Scyllaridae). Mol Phylo Evol **62**(1):237–250. doi:10.1016/j.ympev.2011.09.019.